

Colossal resistive relaxation effects in a $\text{Pr}_{0.67}\text{Ca}_{0.33}\text{MnO}_3$ single crystal

A. Anane,* J.-P. Renard, L. Reversat, C. Dupas, and P. Veillet

Institut d'Electronique Fondamentale, Bâtiment 220, Université Paris-Sud, 91405 Orsay, Cedex, France

M. Viret

Service de Physique de l'Etat Condensé, CEA-Saclay, 91191 Gif-sur-Yvette, Cedex, France

L. Pinsard and A. Revcolevschi

Laboratoire de Chimie des Solides, Bâtiment 414, Université Paris-Sud, 91405 Orsay, Cedex, France

(Received 22 June 1998)

We report here on an experimental study of slow thermal relaxation effects from the metastable metallic-ferromagnetic phase to the insulating one in a charge-ordered manganese oxide, $\text{Pr}_{0.67}\text{Ca}_{0.33}\text{MnO}_3$. The metal-insulator transition is evidenced by an abrupt jump of the resistivity by several orders of magnitude at a well-defined time τ while there is no apparent singularity in the magnetization relaxation. This supports the view of a percolative behavior of current transport. The magnetic relaxation is discussed in terms of a two-level phenomenological model with a distribution of energy barriers.

[S0163-1829(99)00202-7]

Since the observation of the so-called phenomenon of colossal magnetoresistance (CMR) in thin films of mixed-valence Mn perovskites,^{1,2} the interest in these compounds, already studied in the 1950s,³ has been strongly renewed. Indeed, the manganites of general formula $R_{1-x}M_x\text{MnO}_3$ (R = rare earth, M = alkaline earth) exhibit a remarkable behavior in which structural, transport, and magnetic properties are closely and intricately related.⁴

Whereas LaMnO_3 is an insulating antiferromagnet with orbital order between the Mn^{3+} ions, the substituted compounds $\text{La}_{1-x}M_x\text{MnO}_3$ (M = Ca, Sr, Ba), with $x \sim 0.2$ – 0.4 , are metallic ferromagnets which undergo a metal-insulator transition around their Curie temperature, T_c . The CMR effect is simply related to the forced alignment of the Mn magnetic moments by the external field, which allows the easy hopping of carriers between neighboring Mn sites. It is qualitatively explained by the double-exchange mechanism,⁵ but the coupling of charge carriers to phonons is likely to be of importance for quantitative interpretation of the transport properties.⁶ This is supported by the large isotopic effect recently evidenced by the shift of T_c in ^{18}O -enriched $\text{La}_{1-x}\text{Ca}_x\text{MnO}_3$.⁷

In the $R\text{MnO}_3$ perovskites, the double-exchange interaction is mediated by the overlap of the $2p$ orbitals of O and the e_g orbitals of Mn ions that is strongly dependent on the tolerance factor t (where $t = d_{R-O}/\sqrt{2}d_{\text{Mn-O}}$ and d denotes an interatomic distance). Decreasing t leads to an increasing departure from 180° of the Mn-O-Mn angle value, leading to a reduction of the double-exchange transfer integral. This favors the occurrence of an insulating noncollinear Mn spins phase at low temperature with localized carriers. Furthermore, at certain concentrations, this charge localization can be achieved in an orderly way leading to a charge-ordered (CO) phase.

Such a CO phase, originally observed in oxides belonging to high- T_c superconductor families,⁸ was at first proposed to explain the low- T behavior of $\text{Pr}_{0.5}\text{Sr}_{0.5}\text{MnO}_3$ (Ref. 9) and studied in detail in $\text{La}_{0.5}\text{Ca}_{0.5}\text{MnO}_3$.¹⁰ In these manganites, the equal number of Mn ions in the valence states $+3$ and

$+4$ is highly favorable for the establishment of the CO state. However, in manganites with a still smaller tolerance factor, $t \leq 0.91$, the CO state occurs in a relatively wide range of concentrations. In $\text{Pr}_{1-x}\text{Ca}_x\text{MnO}_3$ ($t \cong 0.89$), the CO phase takes place in the range $0.3 \leq x \leq 0.5$ with $T_{\text{CO}} \sim 220$ – 240 K and a relatively complex magnetic phase including antiferromagnetism and/or canted antiferromagnetism has been observed.^{11,12} At low temperature, the application of a magnetic field induces a transition from insulating to metallic phase resulting from the forced alignment of the Mn spins. This phase transition is of first order and the corresponding (T, H) phase diagram displays a strong hysteresis. This hysteresis is especially striking at $x \sim 0.3$ where the field-induced metallic phase is maintained in a metastable state when suppressing the field at $T < 50$ K.¹²

In this paper, we report the first experimental observation of slow dynamical effects at the transition from the metastable metallic phase to the stable insulating CO phase. The experiments were performed on a single crystalline sample of $\text{Pr}_{0.67}\text{Ca}_{0.33}\text{MnO}_3$ cut from a several-cm-long crystal grown in an image furnace by the floating-zone method.^{13,14} All the measurements were carried out on a parallelepiped of size $2 \times 2 \times 8$ mm. The relative Ca/Pr concentration was checked by energy dispersive x-ray analysis in a scanning electron microscope. Four small gold contacts were sputtered on the sample. Electrical resistivity measurements were carried out by the standard four-probe technique, in a variable temperature cryostat (1.4–320 K) equipped with a 10-T superconducting coil. The magnetization of the same sample was measured by superconducting quantum interference device (SQUID) magnetometry.

Resistivity measurements were performed either in fixed applied field versus temperature, or at fixed temperature versus field. In these latter experiments, the sample was first cooled in zero field from room temperature down to the working temperature T_0 . The sample is then set in the insulating antiferromagnetic (AF) phase. At increasing magnetic field up to 10 T, the transition from the insulating AF phase to the metallic ferromagnetic (FM) phase occurs at a well-

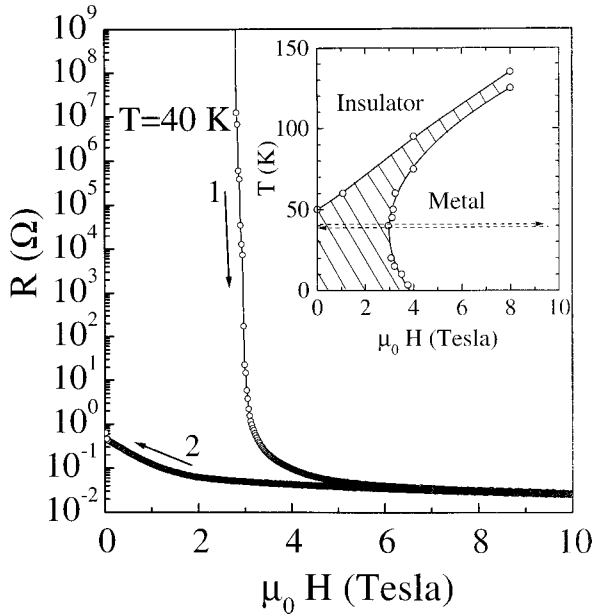


FIG. 1. Resistivity vs magnetic field at $T=40$ K in $\text{Pr}_{0.67}\text{Ca}_{0.33}\text{MnO}_3$ cooled from 300 to 40 K in zero field. The phase diagram in the (H, T) plane is shown in inset. Notice the large hysteresis region (the hatched area) in which the insulating antiferromagnetic and the metallic ferromagnetic phases can coexist.

defined field at which the resistivity drops by several orders of magnitude. This metallic phase is maintained when removing the field at $T_0 \leq 45$ K (Fig. 1). From these experiments, a phase diagram in the (H, T) plane, consistent with that previously established¹² was obtained (Fig. 1). It shows three distinct regions: a first one at high fields and low T where the FM phase sets in, a second one at low fields and high T corresponding to the CO phase, and a hysteresis region limited by two $H(T)$ borderlines, where both phases can be encountered depending on the T or H variation procedure.

Inside the hysteresis region, striking time aftereffects are observed close to the borderlines. These effects were systematically studied at the upper borderline by using the following procedure: after cooling in zero field to a fixed temperature T_0 , the crystal is driven into the metallic state by a 10-T applied field; then the field is quickly decreased (2 T/min) to zero or to a final field H_0 and the resistance R is recorded as a function of time t . Typical $R(t)$ curves, taken either in zero field and at various temperatures T_0 or in various fields H_0 and at $T_0=45$ K, are shown in Figs. 2 and 3. The most salient feature is a sudden jump of the resistance by several orders of magnitude at a well-defined time τ . This transition time from a metallic to an insulating phase exhibits a strong dependence on T_0 and H_0 . The experimental zero-field data are well described by the activation law $\tau = \tau_0 \exp(E_0/k_B T)$ where k_B is the Boltzmann constant, with $\tau_0 = 2.1 \times 10^{-11}$ s and $E_0/k_B = 1380$ K (inset of Fig. 2). The field dependence is also consistent with an $\exp(\mu_0 m H/k_B T)$ activation law (inset of Fig. 3). Finally, all experimental data can be fitted by the following equation [Eq. (1)], which includes both temperature and field dependences:

$$\tau = \tau_0 \exp[(\mu_0 m H + E_0)/k_B T], \quad (1)$$

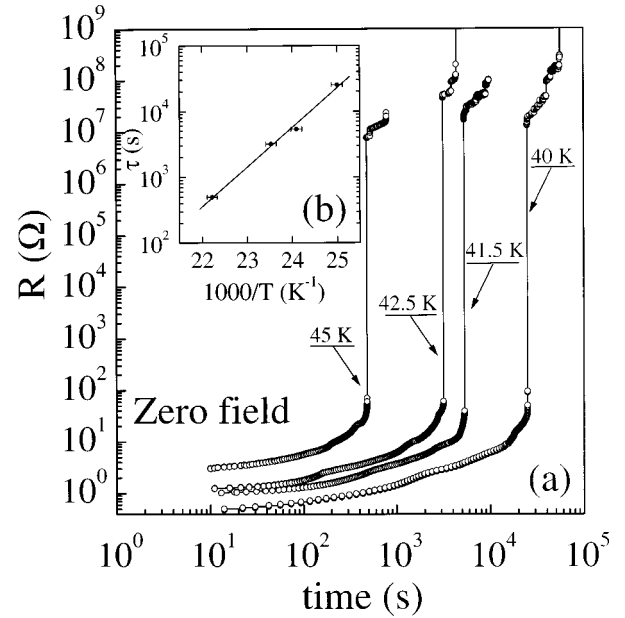


FIG. 2. (a) Logarithmic plot of resistance vs time in zero field and at various temperatures in $\text{Pr}_{0.67}\text{Ca}_{0.33}\text{MnO}_3$. The sample was initially driven into the metastable metallic state by a 10-T applied field (as indicated in the text). (b) Characteristic time τ of the metal-insulator transition in a logarithmic scale as a function of $1000/T$. The straight line is a fit to the activation law $\tau = 2.1 \times 10^{-11} \exp(1380/T)$.

where $m \approx 330 \mu_B$ and $E_0/k_B = 1380$ K. μ_B is the Bohr magneton.

The time dependence of magnetization was investigated on the same sample following a similar procedure. Starting from the metallic phase established at low temperature and high field, here 5.5 T, the sample is quickly driven to a T_0, H_0 point inside the hysteresis region of the phase diagram and the magnetization σ is recorded versus time. Most measurements were carried out at a low-field value, $\mu_0 H_0 = 0.003$ T, and at various temperatures ranging from 35 to 44 K. In addition, a measurement was performed at $\mu_0 H_0 = 0.5$ T and $T_0 = 45$ K in order to provide a direct comparison with the time dependence of resistivity. In all cases, the magnetization was found to decrease slowly with increasing time, the long-time behavior being consistent with a $\log(t)$ linear dependence, often observed in soft ferromagnets¹⁵ and spin glasses.¹⁶ The absolute value of the slope of σ vs $\log(t)$ increases with T but the number of data is insufficient to determine this variation precisely.

The most striking feature is revealed by the comparison of $R(t)$ and $\sigma(t)$ at $\mu_0 H_0 = 0.5$ T; $T_0 = 45$ K. At the time where $R(t)$ changes abruptly by several orders of magnitude, there is no apparent singularity in the magnetization curve (Fig. 4). This strongly suggests that the metastable phase obtained by demagnetizing the crystal at low T is spatially inhomogeneous. It is likely to be composed of a mixture of metallic and insulating regions that may lead to a high electrical conductivity providing that the proportion of ferromagnetic metallic state is large enough to ensure percolation across the sample. Upon increasing time, the proportion of the metallic ferromagnetic phase slowly decreases as shown

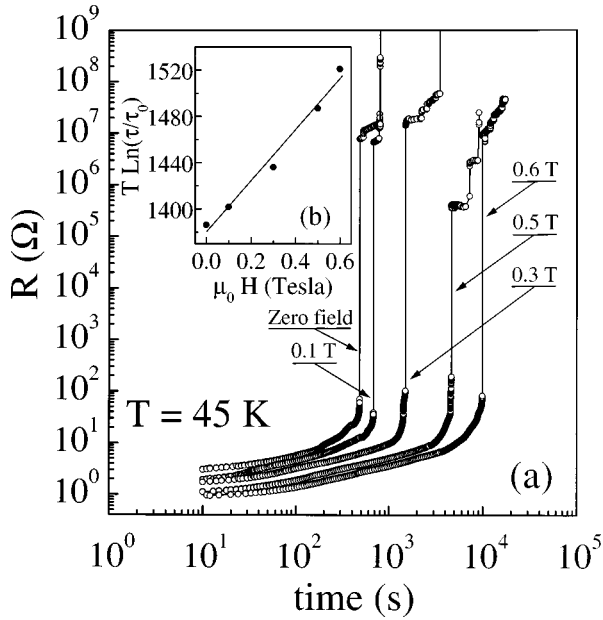


FIG. 3. (a) Logarithmic plot of resistance vs time at $T=45$ K and in various applied fields in $\text{Pr}_{0.67}\text{Ca}_{0.33}\text{MnO}_3$. The sample was initially driven into the metastable metallic state by a 10-T applied field (as indicated in the text). (b) Characteristic time τ of the metal-insulator transition in a logarithmic scale vs applied field H . The straight line is a fit to the activation law $\tau = \tau_0 \exp[(\mu_0 m H + 1380)/T]$.

by the magnetization measurements. When this proportion falls below the percolation threshold, the continuous metallic paths connecting the ends of the sample are suppressed and the resistivity drastically increases.

The temperature dependence of Eq. (1) can be interpreted by a phenomenological model of thermally activated two-level systems, as was previously proposed for the $\text{Nd}_{0.5}\text{Sr}_{0.5}\text{MnO}_3$ system.¹⁷ In this model, the metallic phase and the insulating phase each occupy a minimum in an asymmetrical double well, the lowest minimum being here occupied by the insulating phase. Obviously, only a nonvanishing interaction with the thermal bath enables the system to climb up the energy barrier.¹⁸ In Eq. (1), the τ_0 coefficient is expected to be related to the microscopic mechanism involved in the metal-insulator transition, and therefore should contain the electron-phonon coupling. Recently, the essential role played by the electron-phonon interaction in determining the transport properties of these materials has been clearly evidenced by a huge isotope effect.¹⁹

The effect of an applied magnetic field is to lower the energy of the ferromagnetic metallic phase and, at least for small field values, to increase the height of the energy barrier between the two minima of the well. Clearly, the transition from the metallic to the insulating phase cannot take place in a single step in the whole sample since this would require overcoming a rather high barrier. More likely, one has to consider a collection of a large number of small two-level subsystems with a distribution of energy barriers. The thermally activated transition for a given subsystem should take place at a time longer and longer as the energy barrier is

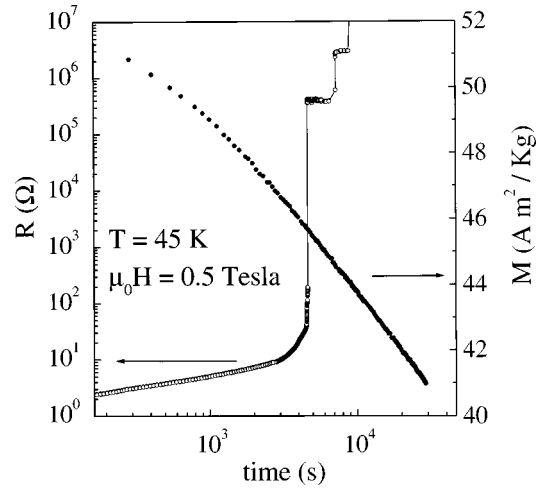


FIG. 4. Comparison between the time dependences of magnetic moment and resistance in $\text{Pr}_{0.67}\text{Ca}_{0.33}\text{MnO}_3$ ($T=45$ K and $\mu_0 H = 0.5$ T). The system was initially driven in the metallic FM phase by a 10-T applied field (as indicated in the text). Notice the absence of any singularity in magnetic moment at the time $\tau=4600$ s, where the resistance jumps by several orders of magnitude.

higher. This is consistent with the continuous slow time decrease of the magnetization. A characteristic size of these subsystems at the percolation threshold could be deduced from the effective magnetic moment m involved in Eq. (1). Expressing it as

$$m = n_{\text{eff}} g \mu_B \langle S \rangle, \quad (2)$$

where $\langle S \rangle$ is the average spin of the Mn ion ($\langle S \rangle = 2 - x/2 = 1.83$) and $g=2$; the experimental m value leads to $n_{\text{eff}} = 90$, which might be interpreted as the number of Mn ions, the transition of which breaks a percolation path at the percolation threshold.

In the present study, the energy barriers are overcome by thermal activation. Recent experiments have evidenced a transition from the insulating to the metallic phase by illumination with x rays at low temperature.²⁰ The stabilization of the metallic phase is somewhat unexpected since its energy is higher than that of the insulating phase in zero field. However, in the frame of the two-level model, a subsystem can overcome the energy barrier by absorption of a high-energy photon and the populations of the two levels tend to equalize by this process. It results that the final proportion of the metallic phase in the sample could reach about one half, which is likely above the percolation threshold and large enough to achieve a low resistivity state.

In summary, we report here the first experimental study of slow thermal relaxation effects at the metal-insulator transition of a charge-ordered manganite. The experimental results support the view of the coexistence of metallic and insulating phases in $\text{Pr}_{1-x}\text{Ca}_x\text{MnO}_3$. The time variation of the resistivity provides evidence for a percolative behavior of current transport. The experimental data are consistent with a simple

phenomenological two-level model with a distribution of energy barriers. A microscopic study by high-resolution imaging techniques would be of great interest to improve the understanding of these phenomena.

This work was supported by the European Commu-

nity Program, Training and Mobility of Researchers, in the frame of the network "Oxide Spin Electronics." The Institut d'Electronique Fondamentale and the Laboratoire des Chimie des Solides are Unités de Recherche Associées au Centre National de Recherche Scientifique No. 22 and No. 446, respectively.

*Corresponding author. Present address: Abdelmadjid Anane, Florida State University, Keen Building, Tallahassee, Florida 32306-3016. FAX: 850-644-6504; Electronic address: anane@martech.fsu.edu

¹R. von Helmolt, J. Wecker, B. Holzapfel, L. Schultz, and K. Samwer, *Phys. Rev. Lett.* **71**, 2331 (1993).

²S. Jin, T. H. Tiefel, M. Mc Cormack, R. A. Fastnacht, R. Ramesh, and L. H. Chen, *Science* **264**, 413 (1994).

³G. H. Jonker and J. H. Van Santen, *Physica (Amsterdam)* **16**, 337 (1950); J. H. Van Santen and G. H. Jonker, *ibid.* **16**, 599 (1950).

⁴For a review, see A. P. Ramirez, *J. Phys.: Condens. Matter* **9**, 8171 (1997) and J. M. D. Coey, M. Viret, and S. von Molnar, *Adv. Phys.* (to be published).

⁵C. Zener, *Phys. Rev.* **81**, 440 (1951); P. W. Anderson and H. Hasegawa, *ibid.* **100**, 675 (1955); P. G. de Gennes, *ibid.* **118**, 141 (1960).

⁶A. J. Millis, P. B. Littlewood, and B. I. Shraiman, *Phys. Rev. Lett.* **74**, 5144 (1995).

⁷G. M. Zhao, K. Conder, H. Keller, and K. A. Mueller, *Nature (London)* **381**, 676 (1996).

⁸C. H. Chen, S. W. Cheong, and A. S. Cooper, *Phys. Rev. Lett.* **71**, 2461 (1993); S. W. Cheong *et al.*, *Phys. Rev. B* **49**, 7088 (1994).

⁹Y. Tomioka, A. Asamitsu, Y. Moritomo, H. Kuwahara, and Y. Tokura, *Phys. Rev. Lett.* **74**, 5108 (1995).

¹⁰P. G. Radaelli, D. E. Cox, M. Marezio, and S. W. Cheong, *Phys. Rev. B* **55**, 3015 (1997), and references therein.

¹¹Z. Jirak, S. Krupicka, Z. Simsa, M. Dlouha, and S. Vratislav, *J. Magn. Magn. Mater.* **53**, 153 (1985).

¹²Y. Tomioka, A. Asamitsu, H. Kuwahara, Y. Morimoto, and Y. Tokura, *J. Phys. Soc. Jpn.* **64**, 3626 (1995); Y. Tomioka, A. Asamitsu, H. Kuwahara, Y. Morimoto, and Y. Tokura, *Phys. Rev. B* **53**, R1689 (1996).

¹³A. Revcolevschi and R. Collongues, *C. R. Seances Acad. Sci., Ser. A* **266**, 1767 (1969).

¹⁴A. Anane *et al.*, *J. Phys.: Condens. Matter* **7**, 7015 (1995).

¹⁵L. Néel, *J. Phys. Radium* **12**, 339 (1951).

¹⁶J. J. Préjean and J. Souletie, *J. Phys. (Paris)* **41**, 1335 (1980).

¹⁷H. Kuwahara, Y. Tomioka, A. Asamitsu, Y. Moritomo, and Y. Tokura, *Science* **270**, 961 (1995).

¹⁸V. I. Melnikov, *Phys. Rep.* **209**, 1 (1991).

¹⁹N. A. Babushkina, L. M. Belova, O. Yu. Gorbenko, A. R. Kaul, A. A. Bosak, V. I. Ozhogin, and K. I. Kugel, *Nature (London)* **391**, 159 (1998).

²⁰V. Kiriukhin, D. Casa, J. P. Hill, B. Keimer, A. Vigliante, Y. Tomioka, and Y. Tokura, *Nature (London)* **386**, 813 (1997).